Hyperreflective Foci in the Inner Nuclear Layer: Proof-of-Concept for an Optical Coherence Tomography Derived Microglia-Related Marker in Multiple Sclerosis

Jonathan A. Gernert, MD,[1,2] Laura M. Bartos, MD,[1,3] Tara Christmann,[1] Hanna Zausinger,[1] Luca N. Diedrich,[1] Daniel Engels, MD, PhD,[1] Miriam Schlüter, MD, PhD,[1] Sarah Schlaeger, MD,[4] Sophia Stoecklein, MD,[4] Leonie F. Keidel, MD,[5] Tania Kümpfel, MD,[1,2,6] Martin Kerschensteiner, MD,[1,2,6] Matthias Brendel, MD, PhD,[3,6,7] and Joachim Havla, MD[1,2]

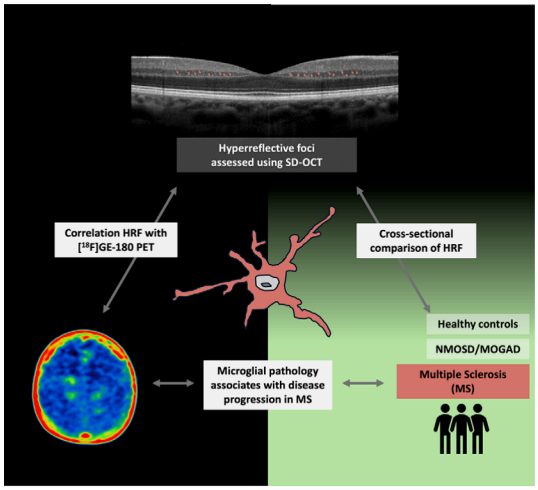

[Color figure can be viewed at www.annalsofneurology.org]

The role of microglia has emerged as a critical driver of disease progression in multiple sclerosis (MS), but we lack broadly applicable monitoring tools. Here, we investigated whether hyperreflective foci (HRF), as detected by optical coherence tomography (OCT) within the inner nuclear layer (INL) of the retina, can be used as a marker for microglial pathology. We demonstrate that HRF counts are increased in persons with relapsing and progressive MS and correlate with global white and gray matter, as well as deep gray matter [^{18}F]GE-180 uptake.

ANN NEUROL 2026;99:1480–1485

Microglial pathology is likely to contribute to progression of relapse-independent disability in persons with multiple sclerosis (PwMS).[1] Measuring this microglial status is thus critical for predicting disease trajectories and monitoring emerging therapeutic interventions.[2] So far, microglial *in vivo* imaging has mainly relied on positron emission tomography (PET) using 18-kDA translocator protein (TSPO) tracers.[1] Although these approaches have shown their clinical potential by detecting rim-active lesions and providing prognostic information on the disease course,[3,4] their accessibility is limited to highly specialized centers and, due to their radiation exposure, they are not well-suited for repeated assessments. Therefore, it is important to develop and validate alternative, more broadly applicable methods to assess microglial pathology. One such low-cost, noninvasive, safe, and easy-to-perform method could be optical coherence tomography (OCT) and more specifically the detection of intraretinal hyperreflective foci (HRF) that have been proposed to correlate with other known markers of microglial origin.[5–7] The histopathological origin of HRF in multiple sclerosis (MS) is under debate and no human histopathological data (with OCT correlation) are available in PwMS. However, there are data from individuals with age-related macular degeneration that show that

From the [1]Institute of Clinical Neuroimmunology, LMU Hospital, Ludwig-Maximilians-Universität München, Munich, Germany; [2]Biomedical Center, Faculty of Medicine, Ludwig-Maximilians-Universität München, Planegg, Germany; [3]Department of Nuclear Medicine, University Hospital of Munich, LMU Munich, Munich, Germany; [4]Department of Radiology, LMU University Hospital, LMU Munich, Munich, Germany; [5]Department of Ophthalmology, Ludwig-Maximilians-University, Munich, Germany; [6]Munich Cluster for Systems Neurology (SyNergy), Munich, Germany; and [7]DZNE-German Center for Neurodegenerative Diseases, Munich, Germany

Address correspondence to Dr Havla, Institute of Clinical Neuroimmunology, NeuroVisionLab, LMU Hospital, Ludwig-Maximilians-Universität München, Munich 81377, Germany. E-mail: joachim.havla@med.uni-muenchen.de

Additional supporting information can be found in the online version of this article.

Received May 5, 2025, and in revised form Feb 19, 2026. Accepted for publication Mar 16, 2026.

View this article online at wileyonlinelibrary.com. DOI: 10.1002/ana.78215.

HRF could also represent melanophages, indicating a histopathological link between HRF and macrophages.[8]

In the present study, we used a robust methodology to count HRF within the inner nuclear layer (HRF_{INL}), compared total HRF_{INL} counts among healthy controls (HC), PwMS, and a mixed NMOSD/MOGAD cohort (aquaporin-4-IgG-positive neuromyelitis optica spectrum disorder/myelin oligodendrocyte glycoprotein antibody-associated disease) and investigated the correlation between total HRF_{INL} counts and [^{18}F]GE-180 uptake in a subgroup of PwMS.

Methods

The LMU Munich ethics committee approved this study (project number: 25-0368-KB) and the German Radiation Protection Committee authorized the study (BfS no. Z 5-22463/2 2015-006). We performed a monocentric, retrospective analysis of individuals from the outpatient clinic of the Institute of Clinical Neuroimmunology at LMU Hospital, Munich. This analysis was conducted according to the Declaration of Helsinki.

We compared the HRF_{INL} counts among the following subgroups: (i) relapsing MS (RMS) and progressive MS (PMS) according to Thompson et al[9]; (ii) NMOSD/MOGAD according to Wingerchuk et al[10] and Banwell et al[11]; and (iii) HC without history of neurological or ophthalmological diseases. Individuals <18 years of age, with $> +5$ diopter (dpt), <-5 dpt, diabetes mellitus, ophthalmological diseases, or a clinical history of optic neuritis (ON) were excluded. Expanded Disability Status Scale (EDSS) is reported as score of clinical disability.

OCT scans were performed during November 2014 to December 2023 using a spectral domain OCT (NeuroVisionLab; Spectralis; Heidelberg Engineering GmbH, Heidelberg, Germany; OCT2-Module). The scan protocol is reported in the Supplementary Material. HRF_{INL} were rated and counted according to current recommendations[12] by three independent experts blinded to demographic and clinical data using all 25 macula scans. If at least 1 of 25 scan was not suitable for HRF_{INL} analysis, the eye was excluded from further analysis. Total HRF_{INL} counts were calculated as $\sum_{j=1}^{25} \text{scan}_j$. Individuals with only one eye suitable for analysis were included, and for individuals whose macula scans were evaluated on both sides, the HRF_{INL} mean count was used.

[^{18}F]GE-180 PET scans were performed at the Department of Nuclear Medicine at LMU Hospital, Munich during April 2016 to February 2020, as previously reported.[13] Magnetic resonance imaging (MRI) scans were performed at the Department of Radiology, LMU Hospital, Munich using a Magnetom Skyra 3T scanner (Siemens, Erlangen, Germany). Please refer to the Supplementary Material for further detailed descriptions on PET and MRI imaging and their analyses.

R software (version 4.4.1; R core team, 2021) was used for statistical analysis. Descriptive statistics are presented as mean ± standard deviation (SD) or median with interquartile range (IQR). The Shapiro–Wilk test was used as test of normality. All statistical tests used are indicated in the Results section in the appropriate place or in the Supplementary Material. Partial correlations adjusted for the time interval between OCT and TSPO-PET examination (in days) were used to assess associations between HRF_{INL} counts and PET imaging parameters. Statistical significance was set at $p < 0.05$.

Results

Initially, an age- and gender-matched cohort of 131 subjects was screened for HRF_{INL} analysis (Supplementary Material). 85 subjects – where at least one eye with all 25 macula scans was suitable for HRF_{INL} analysis – were included for a cross-sectional analysis (see the Table). The pattern of regional distribution of HRF_{INL} was similar across HC, PwMS, and patients with NMOSD/MOGAD with highest mean count in the central region (Fig A, B; see the Table). Using an analysis of covariance (ANCOVA; including gender as cofactor), total HRF_{INL} counts were higher in MS (mean ± SD = 121 ± 43) compared with HC (96 ± 28, $p = 0.029$; Fig C, D). Across the three cohorts, the total HRF_{INL} counts did not correlate with the peripapillary retinal nerve fiber layer (pRNFL) thickness ($r = 0.001$, $p = 0.991$) nor the combined macular ganglion cell and inner plexiform layer (mGCIP) volume ($r = -0.104$, $p = 0.345$) but showed moderate association with the macular INL volume ($r = 0.290$, $p = 0.008$; all Pearson). The total HRF_{INL} counts did not differ between patients with RMS (n = 25, 118 ± 45) or PMS (n = 20, 129 ± 36, $p = 0.374$, unpaired t test). Across all PwMS, the total HRF_{INL} count was not associated with clinical disability (n = 40, EDSS = 2.6 ± 1.5, $r = 0.217$, $p = 0.179$, Pearson). In an explorative subgroup analysis with 9 PwMS, the referenced standardized uptake values (SUVr) of [^{18}F] GE-180 in the global white (WM) ($r = 0.779$, $p = 0.023$), respectively, global gray matter (GM) ($r = 0.821$, $p = 0.013$) and deep gray matter ($r = 0.818$, $p = 0.013$) correlated with the total HRF_{INL} counts (Fig E–H, see the Table; and Supplementary Material).

Discussion

Compared with previous studies on HRF in PwMS, which counted HRF based on a single macular B-scan,[5–7,14] we

TABLE. Demographic and Clinical Data

	HC	MS	NMOSD/MOGAD	*p*
Data on cross-sectional comparison				
Number of subjects, n	23	45	17	
Number of eyes, n	38	75	25	
Gender, Female:Male	14:9	25:20	15:2	**0.050**[a]
Age, year, median (IQR)	43 (32)	41 (17)	47 (15)	0.867[b]
Disease-specific information, n		25 RMS	10 NMOSD	
		20 PMS	7 MOGAD	
EDSS, mean ± SD		2.6 ± 1.5	2.5 ± 2.1	0.888[c]
DMT, yes:no		16:29	9:8	0.254[d]
Total HRF_{INL} count, mean ± SD	95.5 ± 27.6	121.0 ± 43.4	104.0 ± 31.2	**0.038**[e]
m1 HRF_{INL} count, median (IQR)	2.9 (1.9)	3.6 (2.5)	3.0 (2.4)	0.206[f]
m2 HRF_{INL} count, mean ± SD	4.7 ± 1.7	6.0 ± 2.4	5.4 ± 1.7	0.214[g]
m3 HRF_{INL} count, mean ± SD	5.6 ± 1.8	6.5 ± 2.3	6.0 ± 1.8	0.428[g]
m4 HRF_{INL} count, mean ± SD	3.9 ± 1.4	5.0 ± 2.0	4.0 ± 1.7	0.081[g]
m5 HRF_{INL} count, median (IQR)	1.9 (0.9)	2.3 (1.8)	2.0 (0.8)	0.141[f]
Data on PwMS subgroup with TSPO-PET				
Number of subjects, N		9		
Number of eyes, n		17		
Gender, Female:Male		3:6		
Age, year, median (IQR)		49 (15)		
Disease course, N		3 RMS		
		6 PMS		
EDSS, median (IQR)		3.0 (0.75)[h]		
DMT, yes:no		5:4		
Time interval OCT and TSPO-PET examination, days, median (IQR)		81 (65)		
SNP status		4 MAB		
		5 HAB		

Bold values are statistically significance $p < 0.05$.

[a]Fisher's Exact test with $p = 0.04994$. Pairwise comparison using Benjamini–Hochberg: HC vs MS $p = 0.797$; HC vs NMOSD/MOGAD $p = 0.115$; MS vs NMOSD/MOGAD $p = 0.0567$. For further comparisons among the 3 groups, gender was considered as a cofactor due to the (marginal) differences in gender distribution.

[b]Kruskal-Wallis test not significant.

[c]ANOVA test not significant.

[d]Fisher's Exact test not significant.

[e]ANCOVA using gender as cofactor with Bonferroni adjustment: HC vs MS $p = 0.029$; HC vs NMOSD/MOGAD $p = 0.329$; MS vs NMOSD/MOGAD $p = 0.775$.

[f]Kruskal-Wallis test, because the variable was not normally distributed.

[g]ANCOVA using gender as cofactor.

[h]EDSS not available for 2 subjects (N = 7).

DMT = disease modifying therapy; EDSS = expanded disability status scale; HAB = high-affinity binding; HC = healthy controls; HRF = hyperreflective foci (absolute counts, please also refer to the Figure); INL = inner nuclear layer; IQR = interquartile range; MAB = medium-affinity binding; MS = multiple sclerosis; NMOSD = aquaporin 4 antibody-positive neuromyelitis optica spectrum disorder; MOGAD = myelin oligodendrocyte glycoprotein antibody disease; OCT = optical coherence tomography; PMS = progressive multiple sclerosis; Pw = persons with; RMS = relapsing multiple sclerosis; SD = standard deviation; SNP = single-nucleotide polymorphism (rs6971-SNP); TSPO-PET = positron-emission-tomography (PET) scans using the radiotracer [^{18}F]GE-180; n = number

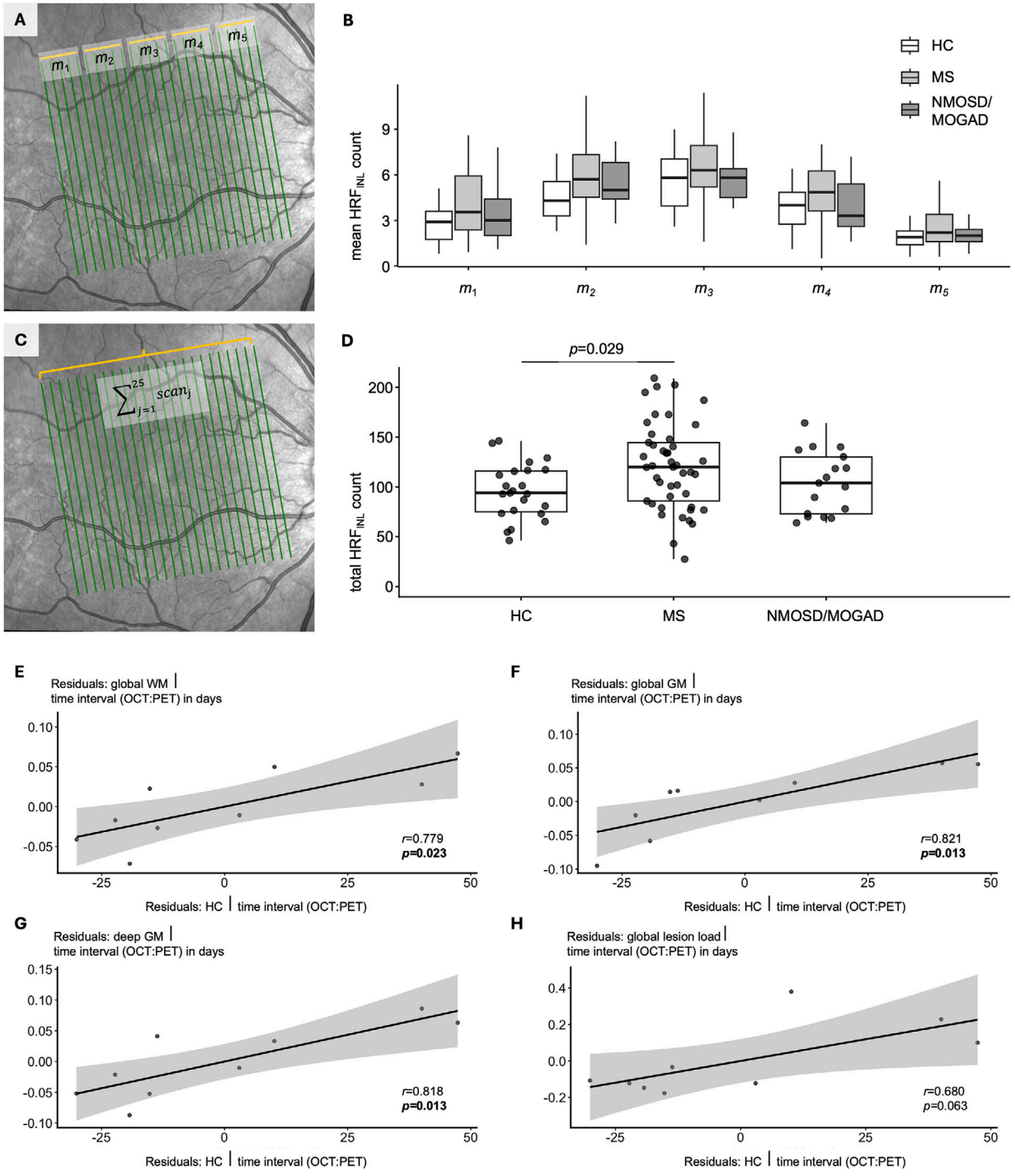

FIGURE: HRF as a potential microglial marker in MS. (A) Macula scan centered to the fovea with 25 B-scans (*green lines*). HRF were manually counted on each B-scan. The B-scans were grouped in 5 sections (*orange lines*) from temporal to nasal (1–5). For each section, mean HRF counts were calculated (m_{1-5}). (B) Boxplots for mean HRF counts within the 5 sections are displayed for 3 groups (white = healthy controls [HC]; light gray = MS; dark gray = NMOSD/MOGAD. Statistical testing for regional distribution across 3 groups is displayed in the Table, comparison analysis within each group is shown in the Supplementary Material. (C) The sum of all HRF was counted across all 25 B-scans per eye (total HRF$_{INL}$ count). (D) Boxplots for total HRF$_{INL}$ counts (with individual measurements as *black dots*) are displayed for the 3 different groups. Statistical analysis is reported in the Table. (E–H) Residual plots for partial correlation between total HRF$_{INL}$ count and SUVr of [^{18}F]GE-180 (corrected for time interval between OCT and PET in days) in global WM (E), global GM (F), deep GM (G), and the global lesional load (H). GM = gray matter; HRF = hyperreflective foci; INL = inner nuclear layer; MOGAD = myelin oligodendrocyte glycoprotein antibody-associated disease; MS = multiple sclerosis; NMOSD = neuromyelitis optica spectrum disorder; OCT = optical coherence tomography; PET = positron emission tomography; SUVr = referenced standardized uptake values; WM = white matter. [Color figure can be viewed at www.annalsofneurology.org]

chose a broader approach by counting the HRF in 25 macula B-scans per eye to minimize the potential impact of possible outliers. With this robust counting method, we were able to trace the regional distribution of HRF_{INL}. Interestingly, we demonstrated that HRF_{INL} are predominantly found in the central area and thus less in the peripheral areas in all 3 groups studied (HC, MS, and NMOSD/MOGAD). Furthermore, our results are consistent with published analyses showing a trend toward higher HRF_{INL} in individuals with MS compared to HC.[5–7,14] In our subgroup analysis, we found comparable HRF_{INL} scores regardless of the disease course of MS. In contrast to our findings, a recent study reported elevated HRF_{INL} values not only in MS but also in NMOSD.[14] These differences may be explained by the following considerations: (i) we included individuals with PMS, respectively, MOGAD; (ii) we excluded eyes with prior ON to reduce possible confounding effects on HRF_{INL} counts; and (iii) additionally, immunotherapies might influence the HRF_{INL} counts. Such effects have been shown, for example, for PwMS.[15] Our results discussed here, are limited by its cross-sectional approach. In the future, multicenter studies with longitudinal OCT examinations are needed to investigate the most reliable and time-effective method for counting HRF. The temporal course of HRF counts after acute ON (in MS, NMOSD, and MOGAD) need to be further studied. In addition, HRF counts in other retinal layers are of high interest since increased HRF counts in the mGCIP and outer nuclear layer (ONL) have been reported in PwMS.[14,16]

The histopathological correlate of HRF in MS is under debate, since, as far as we know, no human comparative studies (OCT and immunohistochemistry) have been published yet. A complicating factor is that HRF are not a static finding, but rather a dynamic one. In principle, previous histopathological data in MS suggest that HLA-DR-positive cells can be found in the INL (and in perivascular areas).[17] On the other hand, OCT examinations in PwMS (especially after excluding individuals with prior ON) demonstrated a correlation with atrophy rates of the global WM, GM, and specific deep GM structures.[18] Therefore, it has been repeatedly concluded that OCT can visualize and monitor global brain pathologies in PwMS. Based on these considerations and data from other ophthalmological diseases, we conducted a correlation analysis between HRF and TSPO-PET. We demonstrated high correlations between HRF and global [^{18}F]GE-180 uptake in WM and GM in a subgroup analysis. The correlation between HRF and [^{18}F]GE-180 uptake in cerebral lesions was borderline but showed a clear trend. Both local (lesion-associated) and global (predominantly in progressive MS) increased TSPO-PET signals have been repeatedly reported.[19] In summary, we add further evidence that HRF_{INL} could be a potential marker for microglia-related pathology, which is thought to be involved as a possible driver of relapse-independent progression in PwMS. However, we would also like to emphasize that the generalizability of our subgroup analysis is limited due to the small number of cases, the heterogeneity of the study, and, not least, the retrospective nature of the analysis. Our results therefore require external validation in larger cohorts, ideally including MRI data (for assessment of paramagnetic rim lesions), and extending the use of other TSPO tracers. Nevertheless, these proof-of-concept data provide evidence that OCT-based detection of HRF_{INL} could serve as a widely accessible, versatile microglia-related marker in PwMS and underscore the importance of retinal imaging in PwMS.

Acknowledgments

This project was partially financed by a research grant of The Sumaira Foundation to J.H. and J.A.G. (SPARK Grant, $25,000). Further, the authors have nothing to report. Open Access funding enabled and organized by Projekt DEAL.

Author Contributions

JAG, MK, MB, and JH contributed to the conception and design of the study; JAG, LMB, TC, HZ, LD, DE, MS, SaS, SoS, LFK, MB, and JH contributed to the acquisition and analysis of data; JAG, LMB, TK, MK, MB, and JH contributed to drafting the text or preparing the figures.

Potential Conflicts of Interest

The authors have nothing to report.

Data Availability

The data of this study are available upon reasonable request to the corresponding author.

References

1. Airas L, Yong VW. Microglia in multiple sclerosis-pathogenesis and imaging. Curr Opin Neurol 2022;35:299–306.

2. Charabati M, Wheeler MA, Weiner HL, Quintana FJ. Multiple sclerosis: Neuroimmune crosstalk and therapeutic targeting. Cell 2023;186:1309–1327.

3. Sucksdorff M, Matilainen M, Tuisku J, et al. Brain TSPO-PET predicts later disease progression independent of relapses in multiple sclerosis. Brain 2020;143:3318–3330.

4. Nylund M, Sucksdorff M, Matilainen M, et al. Phenotyping of multiple sclerosis lesions according to innate immune cell activation using 18 kDa translocator protein-PET. Brain Commun 2022;4:fcab301.

5. Pilotto E, Miante S, Torresin T, et al. Hyperreflective foci in the retina of active relapse-onset multiple sclerosis. Ophthalmology 2020;127: 1774–1776.

6. Pengo M, Miante S, Franciotta S, et al. Retinal Hyperreflecting foci associate with cortical pathology in multiple sclerosis. Neurol Neuroimmunol Neuroinflamm 2022;9:e1180.

7. Puthenparampil M, Torresin T, Franciotta S, et al. Hyper-reflecting foci in multiple sclerosis retina associate with macrophage/microglia-derived cytokines in cerebrospinal fluid. Front Immunol 2022;13: 852183.

8. Augustin S, Lam M, Lavalette S, et al. Melanophages give rise to hyperreflective foci in AMD, a disease-progression marker. J Neuroinflammation 2023;20:28.

9. Thompson AJ, Banwell BL, Barkhof F, et al. Diagnosis of multiple sclerosis: 2017 revisions of the McDonald criteria. Lancet Neurol 2018;17:162–173.

10. Wingerchuk DM, Banwell B, Bennett JL, et al. International consensus diagnostic criteria for neuromyelitis optica spectrum disorders. Neurology 2015;85:177–189.

11. Banwell B, Bennett JL, Marignier R, et al. Diagnosis of myelin oligodendrocyte glycoprotein antibody-associated disease: international MOGAD panel proposed criteria. Lancet Neurol 2023;22:268–282.

12. Vujosevic S, Bini S, Torresin T, et al. HYPERREFLECTIVE RETINAL SPOTS IN NORMAL AND DIABETIC EYES: B-scan and En face spectral domain optical coherence tomography evaluation. Retina 2017;37:1092–1103.

13. Unterrainer M, Mahler C, Vomacka L, et al. TSPO PET with [(18)F]GE-180 sensitively detects focal neuroinflammation in patients with relapsing-remitting multiple sclerosis. Eur J Nucl Med Mol Imaging 2018;45:1423–1431.

14. Klyscz P, Vigiser I, Solorza Buenrostro G, et al. Hyperreflective retinal foci are associated with retinal degeneration after optic neuritis in neuromyelitis optica spectrum disorders and multiple sclerosis. Eur J Neurol 2025;32:e70038.

15. Puthenparampil M, Basili E, Ponzano M, et al. Hyper-reflective foci changes in RRMS under natalizumab therapy. Front Immunol 2024; 15:1421755.

16. Schmidt MF, Pihl-Jensen G, Torm MEW, et al. Hyperreflective dots in the avascular outer retina in relapsing-remitting multiple sclerosis. Mult Scler Relat Disord 2023;72:104617.

17. Green AJ, McQuaid S, Hauser SL, et al. Ocular pathology in multiple sclerosis: retinal atrophy and inflammation irrespective of disease duration. Brain 2010;133:1591–1601.

18. Saidha S, al-Louzi O, Ratchford JN, et al. Optical coherence tomography reflects brain atrophy in multiple sclerosis: a four-year study. Ann Neurol 2015;78:801–813.

19. Guido G, Preziosa P, Filippi M, Rocca MA. TSPO PET in multiple sclerosis: emerging insights into pathophysiology, prognosis, and treatment monitoring. Mult Scler Relat Disord 2025;100:106546.